JOURNAL OF GEOPHYSICAL RESEARCH, VOL. 90, NO. C1, PAGES 975-986, JANUARY 20, 1985

Similarity of the Wind Wave Spectrum in Finite Depth Water
1. Spectral Form

E. BOUWS,[1] H. GÜNTHER,[2] W. ROSENTHAL,[2] AND C. L. VINCENT[3]

A self-similar spectral shape (the TMA spectrum) to describe wind waves in water of finite depth is presented. The parametric spectral form is depth dependent and an extension of the deep water JONSWAP spectrum. The behavior of the spectrum in frequency and wave number space is discussed. About 2800 spectra selected from three data sets (TEXEL storm, MARSEN, ARSLOE) are investigated to show the general validity of the proposal self-similar spectral shape.

1. INTRODUCTION

Wave growth in shallow water seas is not well understood. In deep water, progress in understanding wave growth resulted from observation that the shape of growing wind wave spectra is, to a reasonable degree, regular and can be described by similarity laws [*Phillips*, 1958; *Kitaigorodskii*, 1962; *Pierson and Moskowitz*, 1964; *Hasselmann et al.*, 1973, 1976; *Toba*, 1972]. These spectra show a characteristic development. With growing energy the rather sharp peak migrates toward lower frequencies. The high-frequency flank can be described by a frequency dependence f^{-m}, with m being measured by various groups as lying between 4 and 5. The low-frequency flank is less well known, mainly because energy decreases very rapidly with decreasing frequency and because the observed wind wave records are often contaminated by low-frequency swell. This qualitative description has been quantified, and the parameters descriptive of spectral shape have been related to growth stage parameters such as duration, fetch, and wind speed in order to devise prediction schemes [*Bretschneider and Tamaye*, 1976; *Mitsuyasu*, 1968, 1969; *Hasselmann et al.*, 1973; *Günther et al.*, 1981]. This paper hypothesizes that a description of wave growth in shallow seas may also be approached through similarity principles recognizing the complicating effects of variable water depth and dissipation of wave energy due to the existence of a bottom boundary layer.

At present our understanding of similarity laws for finite-depth wave spectra is analogous to the state of research for deep-water spectra just after the publication of *Phillips* [1958]. The key paper is that of *Kitaigorodskii et al.* [1975], hereafter termed KKZ. In KKZ, Phillips's saturation range concepts for deep-water wave conditions were reexamined and extended to water of finite, constant depth. Here we will propose an application of the KKZ procedure to the entire spectral range, yielding an extension of the self-similar JONSWAP (Joint North Sea Wave Project) shape to finite water depth. The results appear to hold for both flat and gently sloping bottoms. It seems possible to extend the method for other analytical expressions of the spectral shape, such as those proposed by *Toba* [1974] and *Kruseman* [1976]. Based on the KKZ-JONSWAP expression proposed here, it will be possible to develop statistical relationships between finite depth spectral parameters and growth stage parameters. It should be noted that this approach aims to get representative spectra for certain well-defined environmental conditions. A different point of view is taken by *Huang et al.* [1981, 1983]. With the Wallops spectrum model they developed a highly flexible spectral shape, adaptable to various kinds of spectra, even those of a decaying wave field.

The similarity laws of the paper will be checked against data from two large, shallow water wave measurement programs MARSEN (Marine Remote Sensing Experiment at the North Sea) and ARSLOE (Atlantic Ocean Remote Sensing Land-Ocean Experiment) and data from an extreme storm in the southern North Sea collected by Rijkswaterstaat-KNMI. The three data sets will be described in more detail in the next section. They include a variety of wave generation conditions with observations at water depths ranging from 6 to 42 m. Wind speeds in the data set range up to 30 m/s. Bottom conditions range from fine to coarse sands.

The remainder of the paper will be organized in three sections: In section 2 the experiments are described from which observations used in this paper are taken. In section 3, similarity theory for finite-depth wave spectra is reviewed and the proposed spectral shape presented. The viability of the spectral shape is examined against observed spectra. The characteristics of this spectral shape are examined with particular emphasis on variation with water depth. In section 4 we give explicit spectral examples for shallow water wave stations and discuss the determination of the spectral parameters. Also, a statistic is given for the quality of the newly developed depth-dependent spectral shape.

2. EXPERIMENTS

Our work is the result of combining similar elements of three separate studies on shallow-water wind-wave growth that were related to (1) MARSEN, fall 1979; (2) ARSLOE, fall 1980; and (3) a series of measurements of Rijkswaterstaat (RWS) that were processed by KNMI (both in the Netherlands), January 3, 1976. Both MARSEN and ARSLOE were comprehensive experiments with wave measurements forming just one element in both of them. They are similar in that both were aimed at the application of various remote sensing techniques to a number of oceanographic research topics. Another similarity between MARSEN and ARSLOE is the location at a continental shelf with depths up to 40 m. However, there is a difference in the exposure to the deep ocean: MARSEN was located in the southern half of the North Sea, virtually out of reach of the Atlantic Ocean, whereas the ARSLOE site was open to the ocean.

MARSEN

Apart from ocean waves, the MARSEN experiment comprised various subjects, including surface temperatures, cur-

[1] Royal Netherlands Meteorological Institute (KNMI), De Bilt.
[2] Institut für Meereskunde, University of Hamburg and Max-Planck-Institut für Meteorologie, Hamburg, Germany.
[3] Coastal Engineering Research Center, Fort Belvoir, Virginia.

Paper number 4C1001.
0148-0227/85/004C-1001$05.00

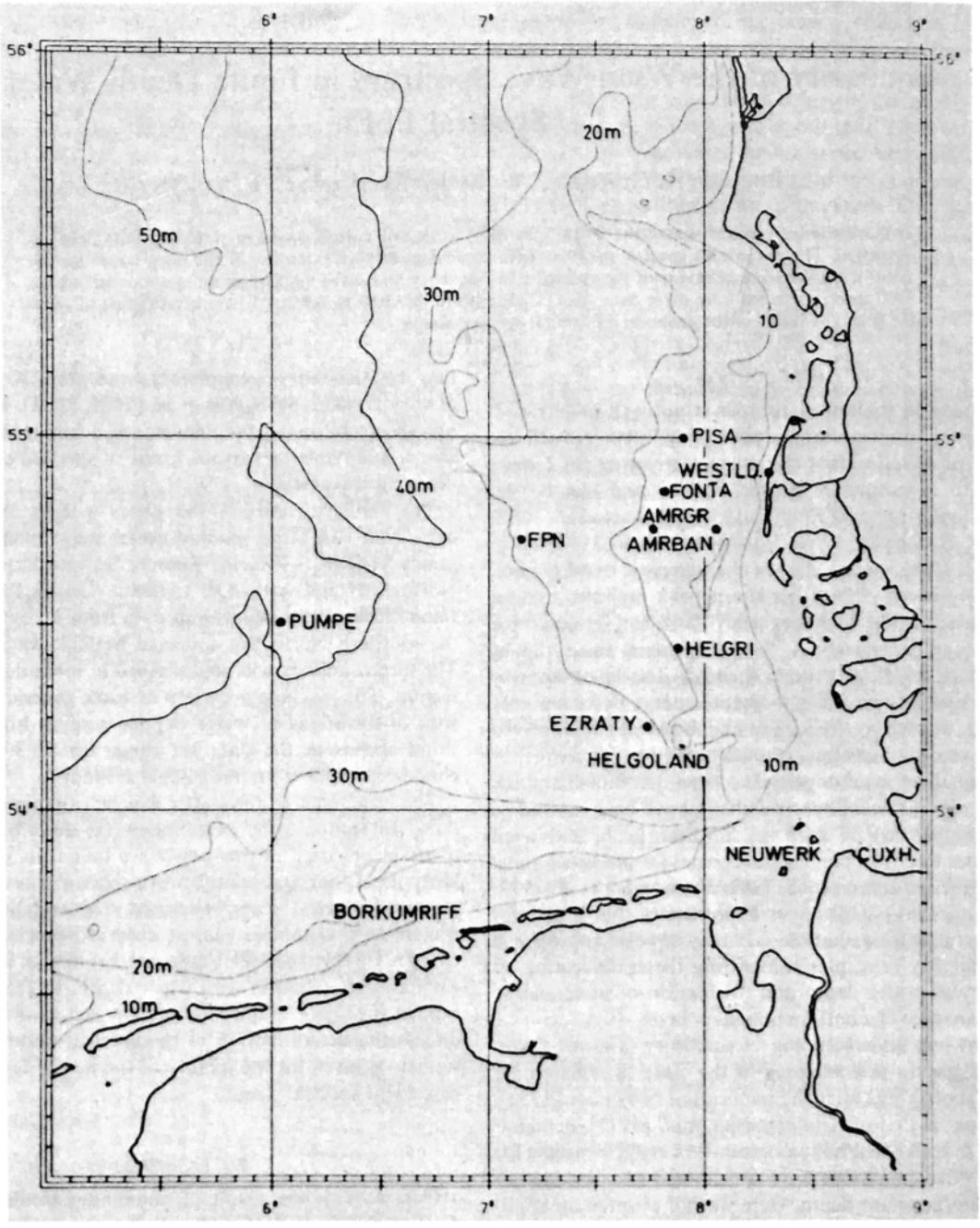

Fig. 1. The bathymetry of the German Bight with MARSEN wave stations used for this study.

rent, and tidal levels. The measurements were aimed at comparisons of various measuring techniques and at the development or improvement of models of shelf-sea circulation, storm surge, and wind waves. Most measurements were located in the German Bight (see Figure 1), some in the Southern Bight (Figure 2). In Figures 1 and 2, only those wave stations selected for this study have been included (see also Table 1). There were nine stations in the German Bight and three stations in the Southern Bight. Fast Fourier transform routines have been used to calculate the spectra with 30 degrees of freedom equivalent to a relative standard error of about 20% following the Bartlett procedure [*Jenkins and Watts*, 1968]. The sample period was 0.5 and the frequency resolution $\Delta f = 1/128$ Hz. Figures 1 and 2 show that the bathymetry was similar in both areas. However, the German Bight is somewhat more exposed to waves entering from the northern North Sea, where the wave climate is approximately the same as in the North Atlantic. To avoid difficulties with inhomogeneous wind data from various sources, e.g., coastal stations may not be representative for the neighboring sea areas under various meteorological conditions, wind directions and wind speeds have been analyzed manually from weather charts for a number of selected periods by Hans Walden.

ARSLOE

This experiment was held between October 6 and November 30, 1980, and is more fully described by *Vincent and Lichy* [1981]. It comprised an oceanfront experiment at the Chesapeake Bay entrance, a terrestrial remote sensing experi-

TABLE 1. List of Wave Stations, Institutes, Types of Instruments, Depths, Dates, and Number of Measurements Used

Data Set	Station Institute	Instrument	Mean Depth, m	Dates	Number of Spectra
MARSEN					
German Bight	WESTLD TUH	WR	6	August–October 1979	57
	AMRBAN DHI	WR	10	August–October 1979	116
	PISA DHI	WR	16	August–October 1979	114
	HELGRI DHI	WR	18	August–October 1979	52
	FONTA IFP	WR	19	August–October 1979	229
	AMRGR DHI	WR	20	August–October 1979	40
	FPN MPI	WS	28	August–October 1979	67
	EZRATY CNEXO	PR	35	August–October 1979	34
	PUMPE CNEXO	WR	42	August–October 1979	53
Southern Bight	NOORDWIJK RWS/KNMI	WS	16	August–October 1979	69
	IJMUIDEN KNMI	WR	25	August–October 1979	45
	K-13-A RWS/KNMI	WR	27	August–October 1979	68
ARSLOE	610	WR	5	October 1980–June 1982	393
	625	WS	9	October 1980–June 1982	382
	620	WR	17	October 1980–June 1982	290
	630	WR	18	October 1980–June 1981	156
	730	WR	22	October 1980–June 1980	144
	720	WR	24	October 1980–June 1980	111
	710	WR	25	October 1980–June 1981	127
	XERB NDBC	PR	36	October 1980–June 1980	270
TEXEL	Euro-5 RWS/KNMI	WR	22	January 3, 1976	5
	LS Texel RWS/KNMI	WR	30	January 3, 1976	19

CNEXO, Centre National pour l'Exploitation des Oceans; DHI, Deutsches Hydrographisches Institut; IFP, Institut Francais du Pétrole; MPI, Max-Planck-Institut für Meteorologie; TUH, Franzius Institut, Universität Hannover; NDBC, U.S. National Data Buoy Center; RWS, Rijkswaterstaat; KNML, Koninklijk Nederlands Meteorologisch Institute.

WR, wave rider; WS, wave staff; PR, pitch-roll buoy.

ment in Elizabeth City, North Carolina, and a wave-measuring experiment aimed at collecting data applicable to a wide variety of investigations of wave mechanics and wave sensor intercomparisons. The primary experimental site was a 30 × 36 km rectangle centered on the CERC Field Research Facility at Duck, North Carolina, and extending from the shore to a depth of about 40 m (see Figure 3). Additionally, data taken after the ARSLOE experiment are also included to increase the data base. Processing of wave data into spectra has been done following the method described by *Harris* [1972]. Most data from the FRF pier have not been included because we confine ourselves to the area largely outside the breaker zone. In most cases this zone was about the offshore end of the pier at a depth of 7–10 m. Wind data were obtained from measurements of the XERB data buoy 36 km offshore at 10-m height. In onshore blowing wind cases these data are representative for the whole area. Since the data from ARSLOE were processed differently from MARSEN, a comparison of spectral analyses was performed and indicated only minor differences in spectral shape.

TEXEL

Various departments of Rijkswaterstaat (RWS) in the Netherlands are measuring waves for operational purposes, both in the field of coastal engineering and navigation. Some of these wave data are collected by KNMI for its wave research, among these a rather unique series of wave rider measurements near lightship *Texel* (Texel) and the Eurochannel (Euro 5) west of Rotterdam harbor (see Figure 2 and Table 1), during a long-lasting northwesterly storm in the central and southern North Sea [cf. *Bouws*, 1980]. The method of calculation of the spectra was similar to that used with the MARSEN data set. Wind data have been obtained from coastal stations; the wind speed has been reduced to 10-m height at sea by correcting for exposure and difference of roughness employing a method by *Wieringa* [1976]. They compare fairly well with the analyses made by *Harding and Binding* [1978] for the North Sea Wave Model Project (NORSWAM).

3. SIMILARITY LAW FOR FINITE-DEPTH WAVES

The shallow-water spectrum will be developed from extension of deep-water similarity principles; those appropriate to the derivation are reviewed below.

The spectrum of actively growing wind waves in deep water can be analytically expressed by the JONSWAP equation [*Hasselmann et al.*, 1973]:

$$E_J(f) = E_p(f)\phi_{PM}(f/f_m)\phi_J(f, f_m, \gamma, \sigma_a, \sigma_b) \quad (1)$$

with

$$E_p(f) = \alpha g^2(2\pi)^{-4} f^{-5} \quad (2)$$

$$\phi_{PM}(f/f_m) = \exp\ -5/4(f/f_m)^{-4} \quad (3)$$

$$\phi_J(f, f_m, \gamma, \sigma_a, \sigma_b) = \exp\ [\ln(\gamma)\exp\ (-(f-f_m)^2/2\sigma^2 f_m^2)] \quad (4)$$

$$g = 9.806\ \text{m s}^{-2}$$

$$\sigma = \begin{cases} \sigma_a & f_m \geq f \\ \sigma_b & f_m < f \end{cases}$$

where E_p is the Phillips equilibrium range formula with a variable coefficient α, ϕ_{PM} is the shape function derived by *Pierson and Moscowitz* [1964] and ϕ_J is the JONSWAP shape

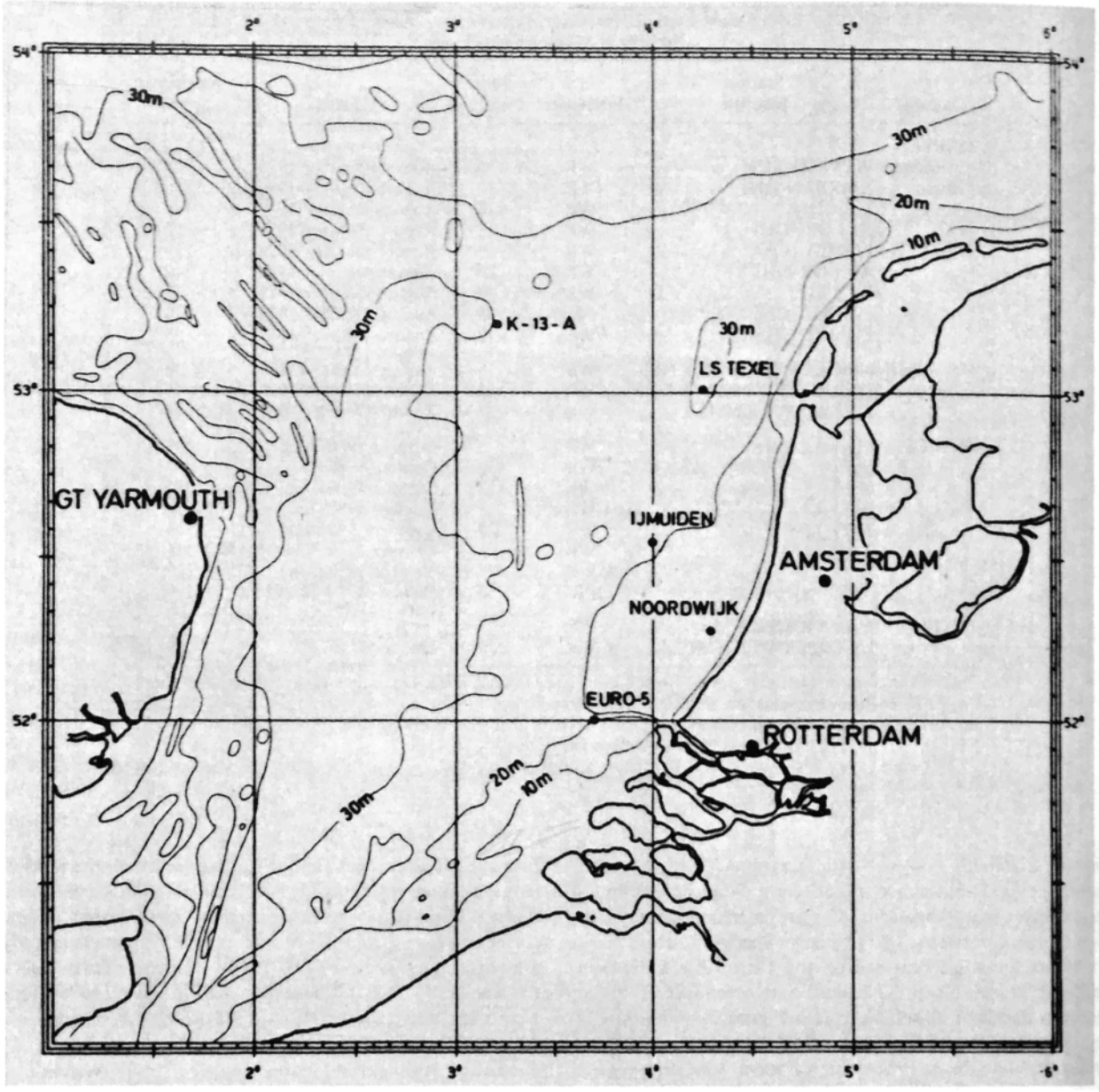

Fig. 2. The bathymetry of the Southern Bight with wave stations used for this study both from MARSEN and from the TEXEL data set.

function. There are other analytical representations that give similar spectral shapes [e.g., *Toba*, 1973; *Kruseman*, 1976; *Huang et al.*, 1980]. Whereas the Kruseman and JONSWAP shape show a f^{-5} decrease for high frequencies, the spectrum proposed by Toba decreases by f^{-4}, while the *Huang et al.* [1981] spectrum frequency dependence is variable. The negative fifth power slope corresponds to that originally proposed by *Phillips* [1958], but a number of recent measurements show the decrease may be better described by a negative fourth power of frequency [e.g., *Kahma*, 1981]. *Forristal* [1981] presents data suggesting both -4 and -5 subranges. In the JONSWAP equation the dependence on frequency is between -5 and -4 in the range between f_m and $2f_m$ because of the factor ϕ_{PM}.

The similarity form in deep water described by (1) or the others is thought to arise due to a balance between atmospheric input, transfers within the spectrum due to resonant

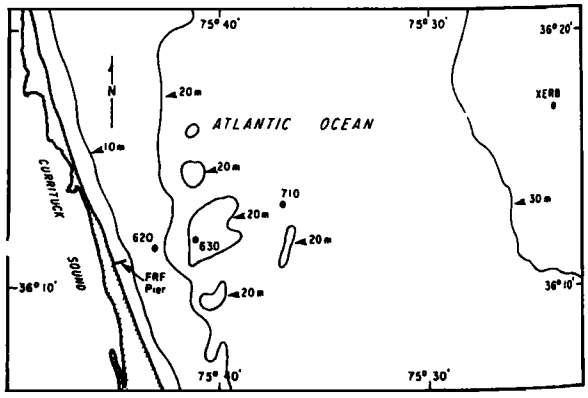

Fig. 3. The bathymetry of the ARSLOE ocean waves experimental site. Also shown are the stations used for this study, except 625 at the FRF pier and 610 in the vicinity of the pier.

nonlinear interactions [*Hasselmann*, 1961; *Hasselmann et al.*, 1973], and dissipation. *Kitaigorodskii* [1983] has suggested that the equilibrium range slope is due to a constant flux of energy through the spectral components arising from the nonlinear interactions.

In shallow water the same processes listed above should be present, though possibly modified by depth (e.g., nonlinear interactions [*Herterich and Hasselmann*, 1980]). Additional processes (bottom friction, percolation, and bottom motion) may be present and highly influenced by depth and site characteristics. Therefore the existence of a similarity law in shallow water is not clear.

However, *Kitaigorodskii et al.* [1975] in KKZ showed that the saturated range of the spectrum in arbitrary depth was given by the one-dimensional spectrum

$$E_K(k, H) = Bk^{-3} \tag{5}$$

with a depth-independent constant B. This may be translated into a one-dimensional frequency spectrum

$$E_K(f, H) = \alpha g^2(2\pi)^{-4} f^{-5} \phi_K(\omega_H) \tag{6}$$

where (see Figure 4)

$$\phi_K(\omega_H) = \frac{\left[(k(\omega, H))^{-3} \dfrac{\partial k(\omega, H)}{\partial f}\right]}{\left[(k(\omega, \infty))^{-3} \dfrac{\partial k(\omega, \infty)}{\partial f}\right]} \tag{7}$$

and

$$\omega_H = 2\pi f(H/g)^{1/2} \tag{8}$$

In deep water this spectrum is the form given by (2) as $E_p(f)$. In shallow water (frequencies with $\omega_H < 1$), (5) has the form

$$E_K(f, H) = \frac{BgH\omega^{-3}}{2} \tag{9}$$

Considerable empirical evidence has accumulated to show $E_K(f, H)$ to be a valid approximation for wind sea cases if α is allowed to vary [*Kitaigorodskii et al.*, 1975; *Vincent et al.*, 1982].

Since the KKZ expression suggests a similarity principle for the saturation range of shallow-water spectrum analogous to the deep-water case, we hypothesize that a shallow-water self-similar shape may be obtained by replacing $E_p(f)$ in (1) with $E_K(f, H)$, yielding

$$E_{TMA}(f, H) = E_K(f, H)\phi_{PM}(f/f_m)\phi_J(f, f_m, \gamma, \sigma) \tag{10}$$

or

$$E_{TMA}(f, H) = E_J(f)\phi_K(\omega_H)$$

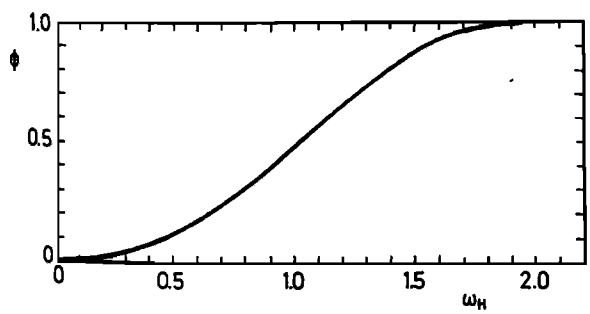

Fig. 4. The transformation factor $\phi(\omega_H)$ defined in equation (12) (reported from KKZ, Figure 1).

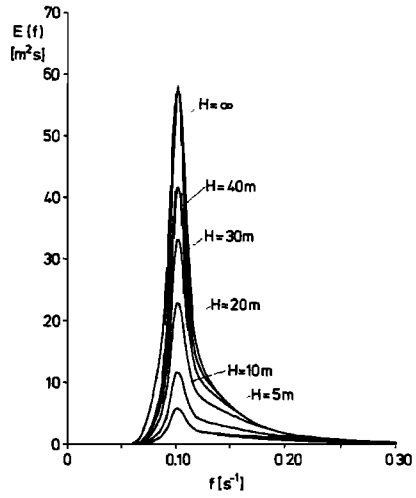

Fig. 5. Self-similar TMA spectra with the same JONSWAP parameters ($f_m = 0.1$ Hz, $\alpha = 0.01$, $\gamma = 3.3$, $\sigma_a = 0.07$, $\sigma_b = 0.09$) for different water depths H.

Since the KKZ has shown that the appropriate scaling is in k space, (10) might be better expressed solely in k space. Since almost all wave observations are made in f space, E_{TMA} is left as expressed (Figures 5 and 6).

The principal hypothesis used to derive E_{TMA} is that the KKZ scaling is not restricted just to the saturation range but is valid across the entire spectrum. This is not novel because the use of the f^{-5} scaling in the JONSWAP, Kruseman, and Pierson-Moskowitz spectra tacitly make this assumption. By the use of the scaling across the entire spectrum we do not imply that any proposed mechanism (such as breaking) dominates the entire spectrum. We simply note that such a scaling has been of practical benefit in specifying deep-water spectra and suggest that it will be useful in shallow water as well.

4. Comparison of the Similarity Law With Field Measurements

We first describe the procedure to derive the spectral parameters from a measured spectrum. Since the fit of the

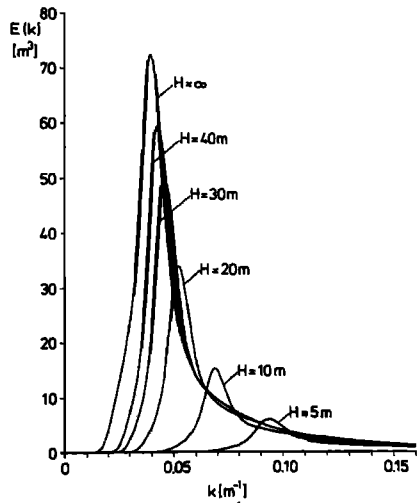

Fig. 6. Same spectra as in Figure 5 but transformed in wave number space.

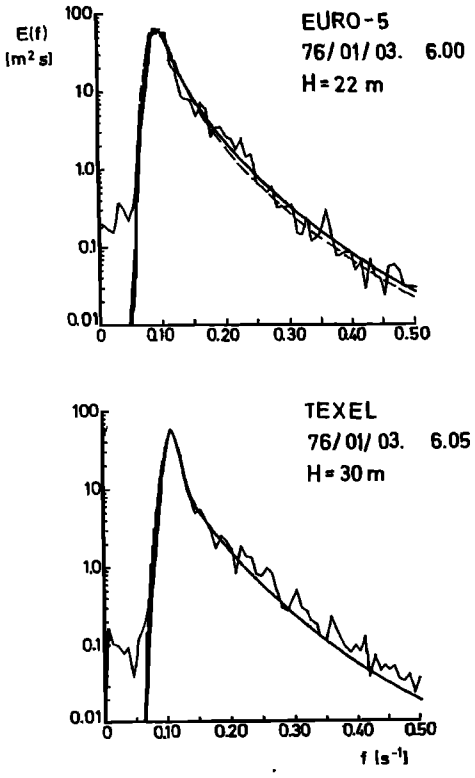

Fig. 7. Comparison of wave spectra from the Rijkswaterstaat-KNMI data set (Southern Bight), with deep-water JONSWAP fit (dashed curve) and finite-depth TMA fit (solid curve). For parameters, see Table 2.

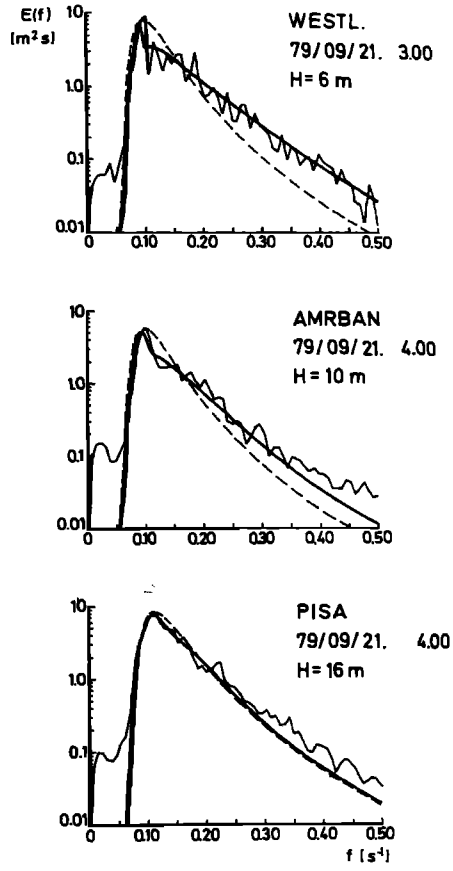

Fig. 8. Same as Figure 7, but spectra form MARSEN (German Bight).

JONSWAP shape for a given deep water spectrum has become routine, we transformed the shallow-water spectra under consideration to the connected deep-water spectrum by multiplying with the reciprocal KKZ factor $\phi_K(\omega_H)$ defined in (7). Subsequently, the deep-water JONSWAP fit described in detail by *Müller* [1976] was applied. Figures 7, 8, and 9 provide examples of the fit of the TMA spectrum to observed spectra. The fit of a JONSWAP deep-water spectrum to each example is also shown. Figure 7 shows two individual cases

TABLE 2. Parameters of Spectra Shown in Figures 7, 8, and 9

Station, Date, Time	Depth, m	Wind Speed, m/s	Wave Height, m	TMA Parameters						
				f_m, s^{-1}	α	γ	σ_a	σ_b	ω_{Hm}	k_mH
EURO-5 January 3, 1976 0600	22	26	6.7	0.089	0.0136	4.18	0.077	0.297	0.85	0.95
TEXEL January 3, 1976 0605	30	26	5.4	0.109	0.0095	7.76	0.120	0.130	1.12	1.26
WESTLD September 21, 1979 0300	6	15	2.7	0.095	0.0135	2.12	0.127	0.058	0.47	0.49
AMRBAN September 21, 1979 0400	10	15	2.3	0.096	0.0056	2.37	0.168	0.065	0.61	0.65
PISA September 21, 1979 0400	16	15	3.2	0.107	0.0096	1.67	0.154	0.163	0.86	0.98
610 October 25, 1980 0835	6	13	3.0	0.092	0.0133	2.68	0.101	0.101	0.45	0.47
630 October 25, 1980 0835	18	13	3.6	0.101	0.0079	5.61	0.065	0.079	0.86	0.98
710 October 25, 1980 0835	25	13	3.6	0.094	0.0069	3.03	0.002	0.084	0.94	1.10

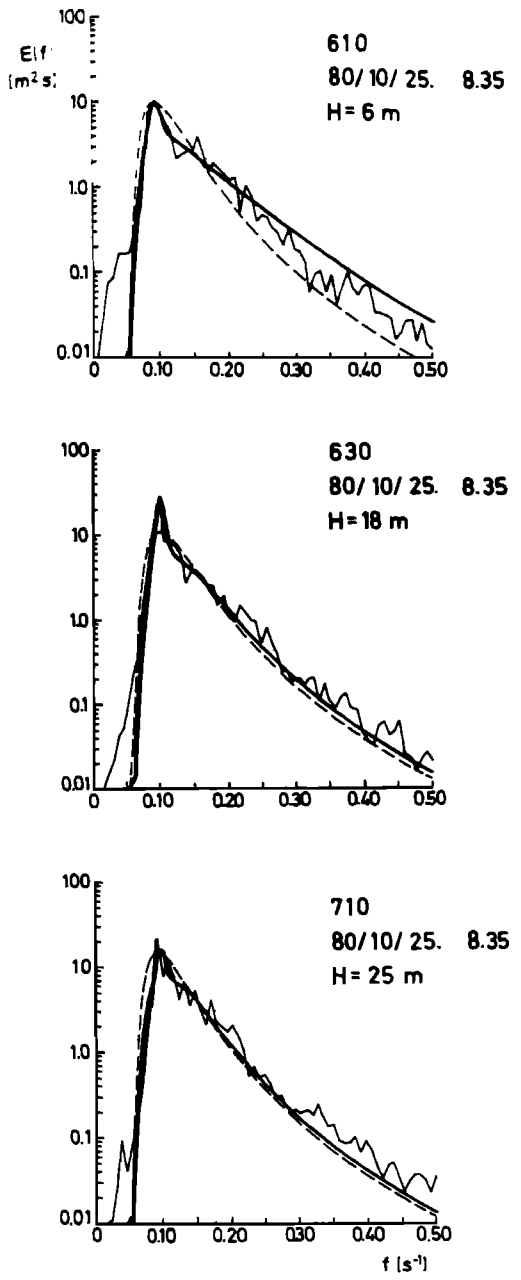

Fig. 9. Same as Figure 7, but spectra form ARSLOE.

from the TEXEL measurements. Figure 8 gives three individual cases from MARSEN, and Figure 9 gives three individual cases from ARSLOE. Table 2 contains the parameters of the spectra from Figure 7 to Figure 9. Visual examination of several hundred examples suggest that the TMA spectrum fits wind wave spectra on finite water depth very well, recognizing that it converges on the deep-water JONSWAP case for deep-water wave spectra.

Since it is not possible to show the quality of the proposed fit for all wind wave spectra of the three data sets, a statistical quality control is derived. The proposed spectral form is written as

$$F(k) = \frac{\alpha}{2} k^{-3} \psi(k, f_m, H) \tag{11}$$

where ψ is the spectral shape function and $\frac{1}{2}\alpha\, k^{-3}$ is the Phillips-Kitaigorodskii scaling factor. $F(k)$ can be envisaged as a basic k^{-3} spectrum up to k_m (defined as the wave number modulus corresponding to the frequency f_m) that is mildly modified at the peak and higher wave numbers by ψ. Below k_m, ψ goes to zero very rapidly. The energy of sea is obtained by

$$E = \int_0^\infty F(k)\, dk = \frac{\alpha}{2} \int_0^\infty k^{-3} \psi(k, f_m, H)\, dk \tag{12}$$

A first approximation to E is obtained by neglecting the contribution of the shape factor ψ

$$E = \frac{\alpha}{2} \int_{k_m}^\infty k^{-3}\, dk \tag{13}$$

Performing the integration yields

$$E = \frac{\alpha}{4} k_m^{-2} \tag{14}$$

This relation was given for deep water already by *Huang et al.* [1980]. In dimensionless form, (14) can be written:

$$\varepsilon = \frac{\alpha}{4} \kappa_m^{-2} \tag{15}$$

where

$$\varepsilon = E \cdot g^2/U^4 \tag{16}$$

is dimensionless energy and

$$\kappa_m = \frac{k_m \cdot U^2}{g} \tag{17}$$

the dimensionless wave number that corresponds to the peak frequency f_m of the TMA spectrum and the depth. This result can be compared to the deep-water JONSWAP result. Using the deep-water relations presented by *Hasselmann et al.* [1976]

$$\varepsilon_\infty = 5.3 \cdot 10^{-6} (f_m U/g)^{-10/3} \tag{18}$$

$$\alpha_\infty = 0.033 (f_m U/g)^{2/3} \tag{19}$$

and the deep-water dispersion relation

$$(2\pi f_m)^2 = g k_m \tag{20}$$

we obtain

$$\varepsilon_\infty = 0.25 \alpha_\infty \kappa_m^{-2} \tag{21}$$

Huang et al. [1981] derived (21) already in their equation (4.4), starting from other statistical relations given by *Hasselmann et al.* [1976].

TABLE 3. Regression Parameters, Their Statistical Uncertainty, and the Standard Deviation of the Data From the Regression Line for the Relation $\varepsilon = A(\alpha\kappa_m^{-2}/B)^r$ With the Normalization Constant $B = 0.0057$

	$A \cdot 10^3$	r	SD, %	Number of Spectra	Figure
All	1.50 ± 0.01	0.88 ± 0.01	25.0	2841	10
$\omega_{Hm} < 0.7$	1.60 ± 0.02	0.89 ± 0.01	24.7	585	11*a*
$0.7 \le \omega_{Hm} < 1.0$	1.57 ± 0.02	0.90 ± 0.01	27.2	619	11*b*
$1.0 \le \omega_{Hm} < 1.3$	1.45 ± 0.01	0.79 ± 0.02	23.6	638	11*c*
$1.3 \le \omega_H$	1.43 ± 0.01	0.87 ± 0.01	22.7	999	11*d*
Equation (24)	1.42	1.0			

B is the mean of $\alpha\kappa_m^{-2}$ for all data.

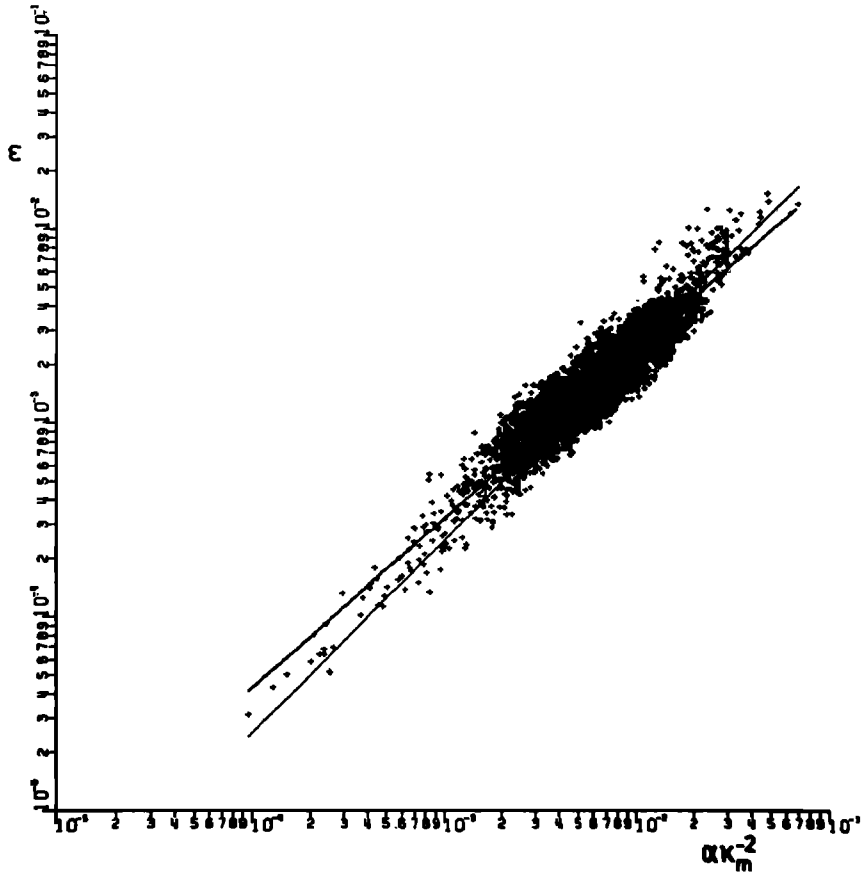

Fig. 10. Dimensionless energy ε versus scaling parameters $\alpha\kappa_m^{-2}$ for the TMA data set. The solid line represents the regression line, the dashed line corresponds to the deep-water relation (24). For regression parameter, see Table 3.

We computed ε, α, and κ_m from the TMA data set and plotted ε versus $\alpha\kappa_m^{-2}$ on a double logarithmic scale. This plot is shown together with the deep-water relation (24) in Figure 10. The fit of the data by a regression line with the fitting parameters r, A

$$\ln \varepsilon = r \ln (\alpha\kappa_m^{-2}/B) + \ln A$$

is shown for comparison with (21). (The normalization constant B is the mean of all data $\alpha\kappa_m^{-2}$ and has the numerical value $B = 0.057$.) The degree to which the regression line has a slope one is a measure of the applicability of the self-similar hypothesis to the entire TMA data set. Figure 10 strongly supports our hypothesis. Further, the data agree with the relationship derived from the deep-water JONSWAP values.

In Figure 11(*a–d*) the data set of Figure 10 is divided into four different classes to show that there exists no systematic depth dependence of the regression. The classes are

$0 \le \omega_{Hm} \le 0.7$	(Figure 11*a*)
$0.7 \le \omega_{Hm} < 1$	(Figure 11*b*)
$1 \le \omega_{Hm} < 1.3$	(Figure 11*c*)
$1.3 \le \omega_{Hm}$	(Figure 11*d*)

where $\omega_{Hm} = 2\pi f_m (H/g)^{1/2}$. The regression parameters of these fits are summarized in Table 3. The statistical uncertainty and the standard deviation are presented, too.

5. Conclusion and Discussion

By extension of KKZ's similarity scaling to the entire spectrum we are led to the proposed finite depth spectral form based on a JONSWAP shape factor. This form gives the JONSWAP spectral shape in deep water and goes to zero for zero water depth. The fits of this proposed spectral form to shallow-water wind-sea spectra are of the same general quality as the fits of the JONSWAP shape are to deep-water spectral observations.

It is possible, based on the assumption of the similarity form, to define a relationship between ε and $\alpha\kappa_m^{-2}$. The plot of observed ε versus $\alpha\kappa_m^{-2}$ (Figures 10 and 11) strongly supports the similarity form hypothesis. This demonstrates that a similarity form exists for the case of growing wind-sea spectrum whether in deep or finite depth water that can be described by one spectral equation. Given the existence of a form with parameters that can be estimated from observations, we shall explore growth-stage relations between them in part 2 of this work.

Although the results of this paper have been expressed mainly in frequency space, the conclusion that wind sea spectra, whether for deep, shallow, or intermediate depth water, can be described by the self-similar TMA spectrum reinforces the conclusion of KKZ that the basic scaling lies in k space. We leave the results in f space notation because most observed or predicted spectra are so expressed.

The spectra examples used here were originally selected as cases of a pure growing wind sea. Care was taken to assure that spectra that might include significant swell components were not included, along with cases in which sudden shifts in winds had recently occurred. Some of such variations may still be in the data and may account for some of the scatter in the diagrams. Other scatter may be due to the ignoring of any

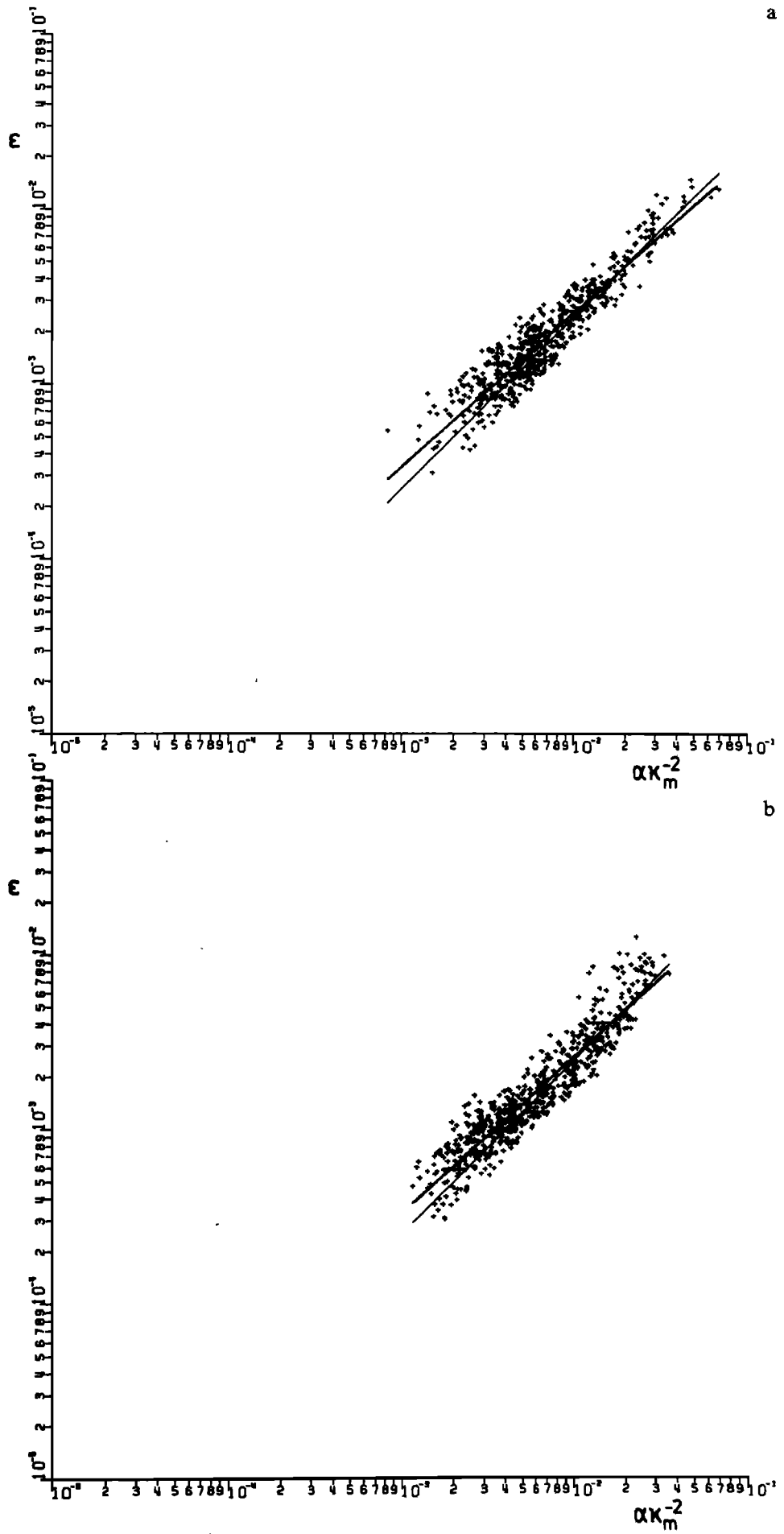

Fig. 11. (*a*) Same as Figure 10, but $0 < \omega_{Hm} < 0.7$. (*b*) Same as Figure 10, but $0.7 \leq \omega_{Hm} < 1.0$. (*c*) Same as Figure 10, but $1.0 \leq \omega_{Hm} < 1.3$. (*d*) Same as Figure 10, but $1.3 \leq \omega_{Hm}$.

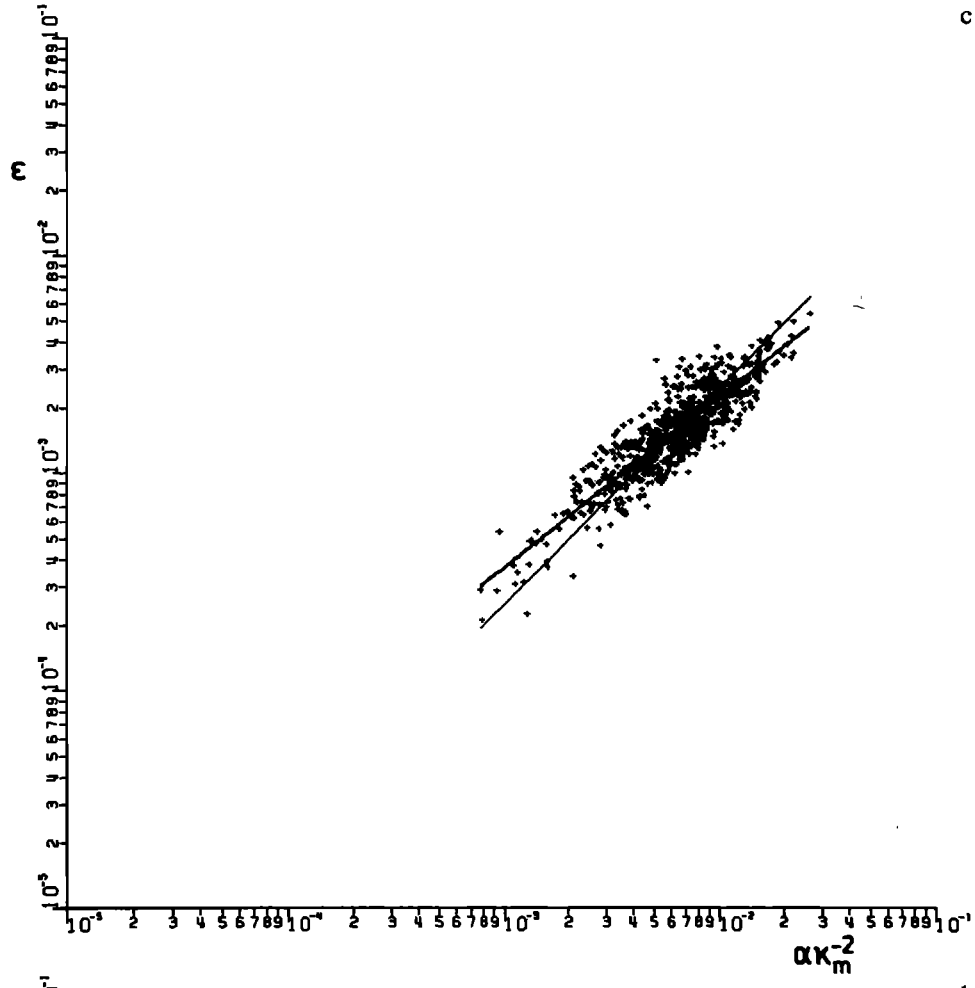

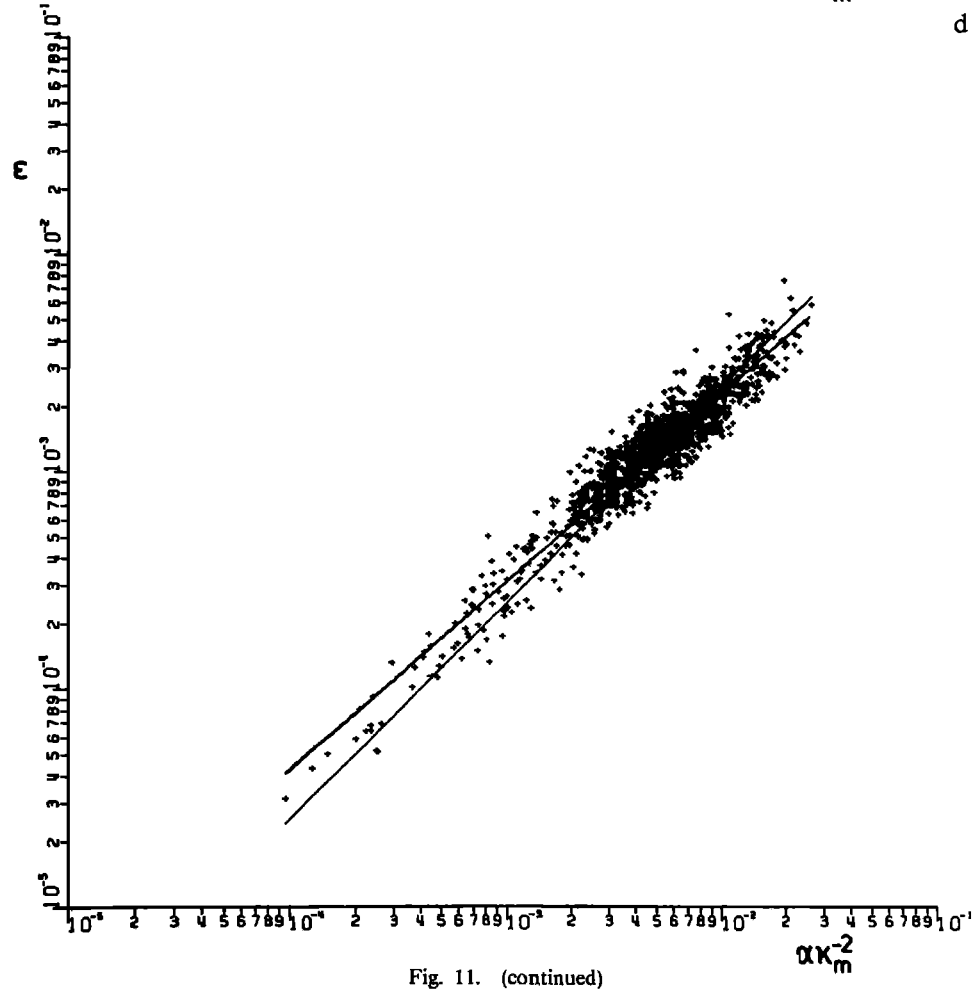

Fig. 11. (continued)

currents that might be present and to the existence of measurement errors.

The TMA spectrum is based on the application of a linear dispersion relation to translate the KKZ k space law into frequency space. By definition it will consist of a smoothly varying single-peak spectrum. Observation and theory support the existence of harmonic Fourier constituents to the principal waves in the spectrum [*Komen*, 1980]; the TMA spectrum makes no attempt to account for the occurrence of these secondary peaks in the region beyond $2f_m$. Although these harmonics are essential to specification of the nonsinusoidal nature of shallow-water waves, they represent a very small part of the variance. At this point we draw no conclusion as to whether the variance in the harmonic range should be considered as real, linear waves or as bound components.

As was mentioned previously, there are other similarity forms, such as that *Toba* [1973] proposed for deep-water wind-sea spectra. *Toba*'s [1973] f^{-4}-law is in fair agreement with the deep-water JONSWAP shape. This means that *Toba*'s [1973] form is not valid in shallow water. It is possible, however, that *Toba*'s [1973] form, like the JONSWAP form, can be converted to a wave number space form, which holds for deep and shallow water. Such an investigation should be performed but is beyond the scope of this paper.

The conclusions that the wind sea spectrum has a self-similar form, irrespective of depth, will be of use in the formulation of prediction models and in engineering design specifications. Beyond its practical utility, self-similarity implies that the relative balance of energy input to the spectrum, dissipation, and transfers within the spectrum is maintained and is constrained to produce a consistent shape.

The hypothesis of a similarity shape has been tested with extensive sets of field data for a range of depths, bottom materials, and wind-generation conditions and appears to hold everywhere. Thus the balance does not appear to be strongly influenced by the nature of bottom conditions, at least over the range examined here. Whether the presence of a predominantly mud bottom, subject to viscoelastic effects, will change this relative balance is unknown. However, the existence of the similarity shape simplifies the problem of understanding the balance of the relatively numerous and complicated source terms by restricting consideration to those combinations that will produce a self-similar shape.

Acknowledgments. For the Dutch part of the work we are grateful to Rijkswaterstaat for providing the raw material to the TEXEL data set and to Roel van Moerkerken (KNMI) for saving this data before anyone else realized its uniqueness. Work at the University of Hamburg was done within the "Sonderforschungsbereich 94," funded by the "Deutsche Forschungsgemeinschaft." We gratefully acknowledge the opportunity to use the data gathered by the participants of the MARSEN 79 experiment, especially to the "Deutsche Hydrographische Institut," which carried out most of the logistics, data collection, and processing during MARSEN. Work performed at the Coastal Engineering Research Center was conducted as part of the Wave Estimation for Design work unit, Coastal Flooding and Storm Protection Program, Coastal Engineering Functional Area, Civil Works Research and Development, U.S. Army Corps of Engineers. Permission to publish these results was granted by the Chief of Engineers. The use of data collected during ARSLOE recognizes the many contributions of the ARSLOE investigators in obtaining these data.

REFERENCES

Bouws, E., Spectra of extreme wave conditions in the Southern North Sea considering the influence of water depth, *Collect. Colloq. Semin. Inst. Fr. Pet.*, *34*, 51–71, 1980.

Bretschneider, C. L., and E. E. Tamaye, Hurricane wind and wave forecasting techniques, paper presented at 15th Coastal Engineering Conference, Am. Soc. Civil Eng., Honolulu, 1976.

Forristall, G. Z., Measurements of a saturated range in ocean wave spectra, *J. Geophys. Res.*, *86*(C9), 8075–8084, 1981.

Günther, H., W. Rosenthal, and M. Dunckel, The response of surface gravity waves to changing wind direction, *J. Phys. Oceanogr.*, *11*, 718–728, 1981.

Harding, J., and A. A. Binding, Windfields during gales in the North Sea and the gales of 3 January 1976, *Meteorol. Mag.*, *107*, 164–181, 1978.

Harris, C. L., Characteristics of wave records in the coastal zone, in *Waves on Beaches and Resulting Sediment Transport*, Academic, New York, 1972.

Hasselmann, K., On the nonlinear energy transfer in a gravity-wave spectrum, 1, General theory, *J. Fluid Mech.*, *12*, 481–500, 1961.

Hasselmann, K., On the spectral dissipation of ocean waves due to whitecapping, *Boundary-Layer Meteorol.*, *6*, 107–127, 1974.

Hasselmann, K., et al., Measurements of wind-wave growth and swell decay during the Joint North Sea Wave Project (JONSWAP), *Deut. Hydrogr. Z., Suppl. A*, *8*(12), 1–95, 1973.

Hasselmann, K., D. B. Ross, P. Müller, and W. Sell, A parametrical wave prediction model, *J. Phys. Oceanogr.*, *6*, 201–228, 1976.

Herterich, K., and K. Hasselmann, A similarity relation for the nonlinear energy transfer in a finite-depth gravity-wave spectrum, *J. Fluid. Mech.*, *97*, 215–224, 1980.

Huang, N. E., S. R. Long, C.-C. Tung, Y. Yuen, and L. F. Bliven, A unified two-parameter wave spectral model for a general sea state, *J. Fluid Mech.*, *112*, 203–224, 1981.

Huang, N. E., P. A. Hwang, H. Wang, S. R. Long, and L. F. Bliven, A study on the spectral models for waves in finite water depth, *J. Geophys. Res.*, *88*(C14), 9579–9587, 1983.

Jenkins, G. M., and D. G. Watts, *Spectral Analysis and Its Applications*, 525 pp., Holden-Day, San Francisco, 1968.

Kahma, K. K., A study of the growth of the wave spectrum with fetch, *J. Phys. Oceanogr.*, *11*, 1503–1515, 1981.

Kitaigorodskii, S. A., Application of the theory of similarity to the analysis of wind-generated wave motion as a stochastic process, *Bull. Acad. Sci. USSR Geophys. Ser.*, *1*, 73, 1962.

Kitaigorodskii, S. A., V. P. Krasitskii, and M. M. Zaslavskii, On Phillips theory of equilibrium range in the spectra of wind-generated gravity waves, *J. Phys. Oceanogr.*, *5*, 410–420, 1975.

Komen, G., Nonlinear contributions to the frequency spectrum of wind-generated water waves, *J. Phys. Oceanogr.*, *10*, 770–790, 1980.

Kruseman, P., Two practical methods of forecasting wave components with periods between 10 and 25 seconds near Hoek van Holland, *Wetensch. Rapp. 76-1*, Kon. Ned. Meteorol. Inst., De Bilt, Netherlands, 1976.

Mitsuyasu, H., On the growth of the spectrum of wind-generated waves, 1, *Rep. 16*, pp. 459–482, Res. Inst. Appl. Mech., Kyushu Univ., Kasuya, 1968.

Mitsuyasu, H., On the growth of the spectrum of wind-generated waves, 2, *Rep. 17*, pp. 235–248, Res. Inst. Appl. Mech., Kyushu Univ., Kasuya, Japan, 1969.

Müller, P., Parametrization of one-dimensional wind waves spectra and their dependence on the state of development, *Hamburger Geophys. Einzelschriften 31*, Geophys. Inst. Univ. Hamburg, Hamburg, Germany, 1976.

Phillips, O. M., The equilibrium range in the spectrum of wind-generated ocean waves, *J. Fluid. Mech.*, *4*, 426–434, 1958.

Pierson, W. J., and L. Moskowitz, A proposed spectral form for fully developed wind seas based on the similarity theory of S. A. Kitaigorodskii, *J. Geophys. Res.*, *69*, 5181–5190, 1964.

Toba, Y., Local balance in the air-sea boundary processes, 1, On the growth process of wind waves, *J. Oceanogr. Soc. Jpn.*, *28*, 109–120, 1972.

Toba, Y., Local balance in the air-sea boundary processes, 3, On the spectrum of wind waves, *J. Oceanogr. Soc. Jpn.*, *29*, 209–220, 1973.

Vincent, C. L., and D. E. Lichy, Wave measurements in ARSLOE, paper presented at Conference on Directional Wave spectra Applications, Am. Soc. Civil Eng., Berkeley, Calif., September 1981.

Vincent, C. L., W. G. Grosskopf, and J. M. McTamany, Transformation of storm wave spectra in shallow water observed during the ARSLOE storm, *Oceans '82*, 920–925, 1982.

Webb, D. J., Nonlinear transfer between sea waves, *Deep-Sea Res.*, *25*, 279–298, 1978.

Wieringa, J., An objective exposure correction method for average wind speeds measured at a sheltered location, *Q. J. R. Meteorol. Soc.*, *102*, 242–253, 1976.

World Meteorological Organization, Handbook on Wave Analysis and Forecasting, *WMO 446*, Geneva, 1976.

E. Bouws, Royal Netherlands Meteorological Institute (KNMI), De Bilt, The Netherlands.

H. Günther and W. Rosenthal, Institut für Meereskunde, University of Hamburg and Max-Planck-Institut für Meteorologie, Hamburg, Germany.

C. L. Vincent, Coastal Engineering Research Center, Fort Belvoir, VA 22060.

(Received March 13, 1984;
accepted June 12, 1984.)